Int. J. ITS Res. (2010) 8:1–9
DOI 10.1007/s13177-009-0005-x

Traction Control for EV Based on Maximum Transmissible Torque Estimation

Dejun Yin · Yoichi Hori

Received: 10 March 2009 / Revised: 5 October 2009 / Accepted: 12 October 2009 / Published online: 20 January 2010

Abstract Research on motion control of EVs has progressed considerably, but traction control has not been so sophisticated and practical because the velocity of vehicles and the friction force are immeasurable. This work takes advantage of the features of driving motors to estimate the maximum transmissible torque output in real time based on a purely kinematic relationship, and then proposes an innovative controller to follow the estimated value directly and constrain the torque reference for slip prevention. By comparison with prior control methods, the resulting control design approach is shown to be more effective and robust both in simulation and on an experimental EV.

Keywords Electric vehicle · Traction control · Slip prevention · Sensorless · Maximum transmissible torque estimation

1 Introduction

Traction control, as a primary control for vehicles, is developed to ensure the effectiveness of the torque output. The key to traction control is antislip control, especially for light vehicles because they are more inclined to skid on slippery roads. A severe slip between the tire and the road surface will not only decrease the longitudinal friction force that accelerates or decelerates the vehicle, but also incur a quick loss on the lateral friction force, which seriously impairs the steering performance. Traction control must not only guarantee the effectiveness of the torque output to maintain vehicle stability, but also provide some information about tire-road conditions to other vehicle control systems. Based on the core traction control, more complicated two-dimension motion control for vehicles can be synthesized by introduction of some information on steering angle, yaw rate, etc. Moreover, from the viewpoint of the relation between safety and cost, a more advanced traction control synthesis also means lower energy consumption. Traction control can also contribute to intelligent transport systems (ITS) [1–4]. For example, in the system of BMW's Connect Drive [5, 6], a smart traction control can detect the road friction and share this information with other vehicles in this network by car-to-car communication, which can make up a continuously updating road-condition map of some area.

Considering the difficulty in directly detecting the road condition, conventional traction control is dependent on the slip ratio reference to perform wheel control. For this reason, up to now, conventional traction control methods have been, with a great deal of effort, seeking to calculate or measure the chassis velocity as a way of making use of the slip ratio in the nonlinear tire model, e.g. Magic Formula [7], to get the maximum friction force from the tire-road surface.

However, actual vehicles present challenges to these types of traction control. In conventional traction control systems, due to physical and economic reasons, the non-driven wheels are ordinarily utilized to provide an approximate vehicle velocity. However, this method is not applicable when the vehicle is accelerated by 4WD systems or decelerated by

D. Yin (✉)
Department of Electrical Engineering, University of Tokyo,
Room Ce-503, 4-6-1 Komaba,
Meguro, Tokyo 153-8505, Japan
e-mail: yin@horilab.iis.u-tokyo.ac.jp

Y. Hori
Institute of Industrial Science, University of Tokyo,
Room Ce-501, 4-6-1 Komaba,
Meguro, Tokyo 153-8505, Japan
e-mail: hori@iis.u-tokyo.ac.jp

brakes equipped in these wheels. Therefore, in some experimental environments, a fifth wheel equipped with rotational speed sensors is usually used to detect the chassis velocity. Accelerometer measurement is also used to calculate the velocity value, but in this case offset and error problems are unavoidable. In particular, when a vehicle drives on a slope, the accelerometer cannot distinguish whether the acquired value results from the acceleration or the component of gravity. Other sensors, e.g., optical sensors [8], sensors of magnetic markers and so on can also be used to obtain the chassis velocity [9, 10]. Although these types of sensor can provide a very high precision of the absolute chassis velocity against the road surface, besides requiring fine maintenance, they are too sensitive and reliant on the driving environment to be applied in actual vehicles.

However, the advantages of EV offer some new approaches to this problem, as well as to the global problems of the environment and non-renewable resources [10–13]. From the viewpoint of motion control, compared with internal combustion engine vehicles, the advantages of EVs can be summarized as follows [14]:

1) Quick torque generation
2) Easy torque measurement
3) Independently equipped motors for each wheel

The torque output of the motor can be easily calculated from the motor current. This merit makes it easy to estimate the driving or braking force between the tire and road surface in real time, which contributes a great deal to application of new control strategies based on road condition estimation. The independently equipped motors provide higher power/weight density, higher redundancy for safety and better dynamic performance [15, 16].

Some controllers, for example the antislip control system based on Model Following Control (MFC), making use of the advantages of EVs, do not need information on chassis velocity or even acceleration sensors. In these systems, the controllers only make use of torque and wheel rotation as input variables for calculation. Fewer sensors contribute not only to lower cost, but also higher reliability and greater independence from driving conditions, which are the most outstanding merits of this class of control systems. Accordingly, research on more practical and more sophisticated antislip control based on MFC continues until now. Sakai et al. proposed a primary MFC system for antislip control [17]. In their inspiring papers, Saito et al. modified it and proposed a novel stability analysis to decide the maximum feedback gain, and furthermore, took the antislip control as a core subsystem and extended it to two-dimension motion control [18, 19]. Akiba et al. improved the control performance by introduction of back electromotive force, and added a conditional limiter to avoid some of its inherent drawbacks [20]. Nevertheless, these control designs based on compensation have to consider the worst stability case to decide the compensation gain, which impairs the performance of antislip control. Furthermore, gain tuning for some specific tire-road conditions also limits the practicability of this method.

Therefore, this paper, making use of the advantages of EVs, focuses on development of a core traction control system based on Maximum Transmissible Torque Estimation (MTTE) that requires neither chassis velocity nor information about tire-road conditions. In this system, use is made of only the torque reference and the wheel rotation to estimate the maximum transmissible torque to the road surface, then the estimated torque is applied for antislip control implementation.

The rest of the paper is structured as follows. "COMS3-experimental EV" describes an EV modified for experiments. "MTTE and antislip control" presents a longitudinal model of vehicles, and analyzes the features of antislip control. MTTE and a control algorithm based on it are then proposed. Comparing with a prior antislip control, "Experiments and simulation" demonstrates simulations and experiments. A detailed discussion follows in "Discussion", analyzing the features of the proposed control method with a partially linearized vehicle model.

2 COMS3-experimental EV

In order to implement and verify the proposed control system, a commercial EV, COMS, which is made by TOYOTA AUTO BODY Co. Ltd., shown in Fig. 1 was modified to fulfill the experiments' requirements. Each rear wheel is equipped with an Interior Permanent Magnet Synchronous Motor (IPMSM) and can be controlled independently.

As illustrated in Fig. 2, a control computer was added to take the place of the previous ECU to operate the motion control. The computer receives the acceleration reference signal from the acceleration pedal sensor, the forward/backward signal from the shift switch and the wheel

Fig. 1 A new experimental EV

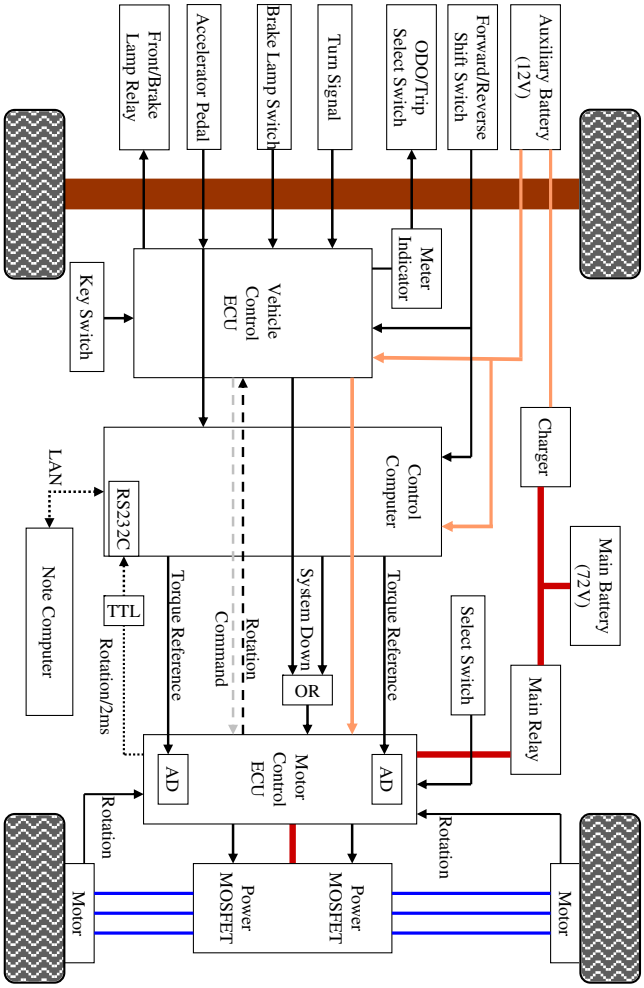

Fig. 2 Electrical System of COMS3

rotation from the inverter. Then, the calculated torque reference of the left and the right rear wheel are independently sent to the inverter by two analog signal lines. Table 1 lists the main specifications.

The most outstanding feature of the modified inverter is that the minimum refresh time of the torque reference is decreased from 10 ms to 2 ms, which makes it possible to actualize the torque reference more quickly and accurately. The increased maximum rate of change of the torque reference permits faster torque variation for high performance motion control.

Table 1 Specification of COMS3.

Total weight	360 kg
Max. power	2,000 W×2 (Rated value: 290 W×2)
Max. torque	100 Nm×2 (Rated value: 10 Nm×2)
Wheel inertia	0.5kgm^2×2
Wheel radius	0.22 m
Sampling time	0.01 s
Controller	PentiumM 1.8G, 1 GB RAM
A/D and D/A	12 bit
Shaft encoder	36 pulse/round

3 MTTE and antislip control

3.1 Longitudinal model and dynamic analysis

Because only longitudinal motion is discussed in this paper, the dynamic longitudinal model of the vehicle can be described by Fig. 3, and the parameter definitions are listed in Table 2.

Generally, the dynamic differential equations for the calculation of longitudinal motion of the vehicle are described as follows:

$$J_w \dot{\omega} = T - rF_d \tag{1}$$

$$M\dot{V} = F_d - F_{dr} \tag{2}$$

$$V_w = r\omega \tag{3}$$

$$F_d = \mu(\lambda)N \tag{4}$$

$$\lambda = \frac{V_w - V}{V_w} \tag{5}$$

The interrelationships between the slip ratio and friction coefficient can be described by various formulas. Here, as shown in Fig. 4, the widely adopted Magic Formula is applied to build the vehicle model for the following simulations. Figure 5 provides some typical μ-λ curves.

3.2 Maximum transmissible torque estimation

In this paper, in order to avoid the complicated μ-λ relation, only the dynamic relation between tire and chassis is considered based on the following considerations, which

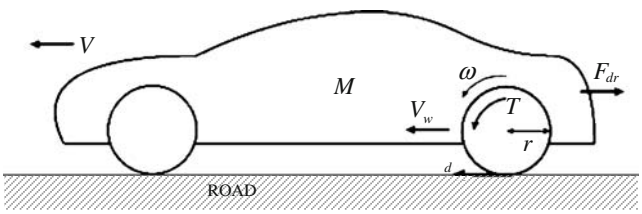

Fig. 3 Dynamic longitudinal vehicle model

Table 2 Parameter list.

Symbol	Definition
J_w	Wheel inertia (motor included)
V_w	Wheel velocity (circumferential velocity)
ω	Wheel rotation
T	Driving torque
r	Wheel radius
F_d	Friction force (driving force)
M	Vehicle mass
N	Vehicle weight
V	Chassis velocity (vehicle velocity)
F_{dr}	Driving resistance
λ	Slip ratio
μ	Friction coefficient

transform the antislip control into maximum transmissible torque control.

1) Whatever kind of tire-road condition the vehicle is driven in, the kinematic relationship between the wheel and the chassis is always fixed and known.
2) During the acceleration phase, considering stability and tire adhesion, well-managed control of the velocity difference between wheel and chassis is more important than the mere pursuit of absolute maximum acceleration.
3) If the wheel and the chassis accelerations are well controlled, the difference between the wheel and the chassis velocities, i.e. the slip is also well controlled.

According to (1) and (3), the driving force, i.e. the friction force between the tire and the road surface, can be calculated as (6). Assuming T is constant, it can be found that the higher the acceleration of ω, the lower F_d. In normal road conditions, F_d is less than the maximum friction force from the road and increases as T goes up. However, when slip occurs, F_d equals the maximum friction force that the tire-road relation can provide and cannot increase with T. Here, there are only two parameters,

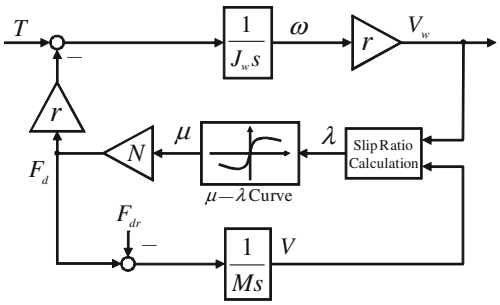

Fig. 4 One-wheel vehicle model

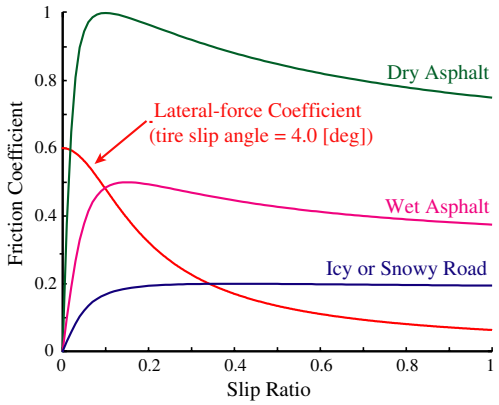

Fig. 5 Typical μ-λ *curves*

r and J_w, so F_d is easily calculated in most tire-road conditions.

$$F_d = \frac{T - J_w \dot{\omega}}{r} \tag{6}$$

When slip starts to occur, the difference between the velocities of the wheel and the chassis becomes larger and larger, i.e. the acceleration of the wheel is larger than that of the chassis. Furthermore, according to the Magic Formula, the difference between the accelerations will increase with the slip.

Therefore, the condition that the slip does not start or become more severe is that the acceleration of the wheel is close to that of the chassis. Moreover, considering the μ-λ relation described in the Magic Formula, an appropriate difference between chassis velocity and wheel velocity is necessary to provide the friction force. Accordingly, (7) defines α as a relaxation factor to describe the approximation between the accelerations of the chassis and the wheel. In order to satisfy the condition that slip does not occur or become larger, α should be close to 1.

$$\alpha = \frac{\dot{V}^*}{\dot{V}_w^*}, \text{ i.e. } \alpha = \frac{(F_d - F_{dr})/M}{(T_{\max} - rF_d)r/J_w} \tag{7}$$

With a fixed α, when the vehicle enters a slippery road, $T_{\max}$ must be reduced adaptively following the decrease of F_d to satisfy (7), the no-slip condition.

Since the friction force from the road is available from (6), the maximum transmissible torque, $T_{\max}$ can be calculated as in (8). This formula indicates that a given F_d allows a certain maximum torque output from the wheel so as not to increase the slip. Here, it must be pointed out that driving resistance, F_{dr} is assumed to be 0, which will result in an over evaluation of $T_{\max}$ and consequently impair the antislip performance.

$$T_{\max} = \left(\frac{J_w}{\alpha M r^2} + 1\right) r F_d \tag{8}$$

Finally, the proposed controller can use $T_{\max}$ to constrain the torque reference if necessary.

3.3 Controller design

The torque controller is designed as in Fig. 6, in which the limiter with a variable saturation value is expected to realize the control of torque output according to the dynamic situation. Under normal conditions, T^*, the torque reference from accelerator pedal or upper controller, is expected to pass through the controller without any effect. On the other hand, when on a slippery road, the controller can constrain the torque output to be close to $T_{\max}$.

First, the estimator uses the driving torque generated by inverter-motor system and the rotation speed of the wheel to calculate the friction force, and then estimates the maximum transmissible torque according to (8). Finally, the controller utilizes the estimated torque value as a saturation value to limit the torque reference. In essence, the estimation shown in Fig. 6 is a disturbance observer.

Here, although it will cause some phase shift, due to the low resolution of the shaft encoder installed in the wheel, a low pass filter (LPF) with a time constant of τ_1 is introduced to smooth the digital signal, ω, for the differentiator which follows. In order to keep the filtered signals in phase, another LPF with a time constant of τ_2 is added for T. The more precise the shaft encoders are, the smaller the time constants are.

In real experiments, even in normal road conditions, $T_{\max}$ may be smaller than T^* due to system delay at the beginning of acceleration, which will cause suddenly commanded acceleration to be temporarily constrained by $T_{\max}$ during the acceleration phase. In order to avoid this problem, as shown in Fig. 7, the increasing rate of T^* is amplified as a stimulation to force the under-evaluated $T_{\max}$ to meet the acceleration reference. Here, $T'_{\max}$ is used instead of $T_{\max}$ as the input to the controller, whose relation

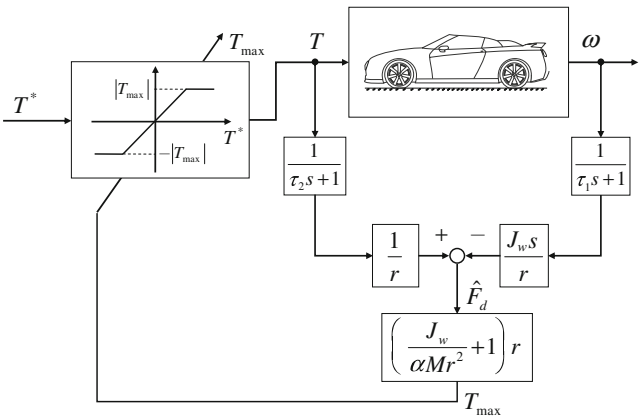

Fig. 6 Control system based on MTTE

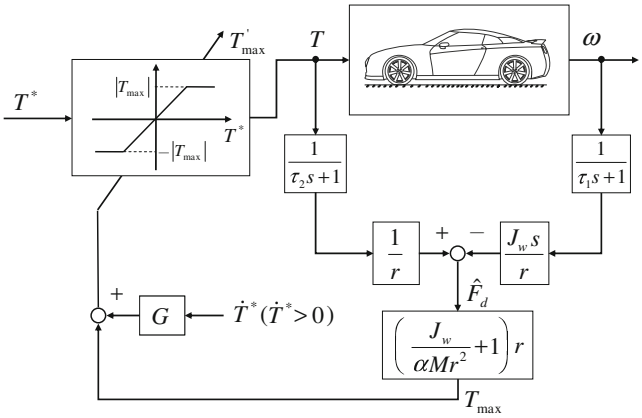

Fig. 7 Control system with acceleration compensation

is described by (9). Here, G is a compensation gain. Additionally, the over-amplified $T'_{\max}$ can be automatically constrained by the following controller. In the following experiments, G was set to 0.1.

$$T'_{\max} = T_{\max} + \dot{T}^* G\left(\dot{T}^* > 0\right) \tag{9}$$

4 Experiments and simulation

This paper uses the antislip control system based on MFC presented in [18] and [19], shown in Fig. 8, for the following comparison. In the following experiments, the same parameters of the vehicle are adopted and the feedback gain in the MFC, K_m is set to the maximum value that ensures the best control performance while maintaining system stability. In the control based on MTTE, α is fixed as 0.9 to pursue a good antislip performance, and τ_1=τ_2=50 ms [21]. The time constant in MFC is set to 50 ms.

Controllers designed as in Figs. 7 and 8 were applied to COMS3 for experiments. In these experiments, the slippery road was simulated by an acrylic sheet with a length of 1.2 m and lubricated with water. The initial velocity of the vehicle was set higher than 1 m/s to avoid the immeasurable zone of the shaft sensors installed in the wheels. Here,

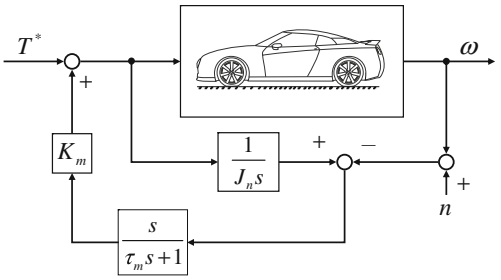

Fig. 8 Block diagram of traction control based on MFC

it must be pointed out that in order to detect the chassis velocity, only the left rear wheel is driven by the motor, while the right rear wheel rolls freely to provide a reference value of the chassis velocity for comparison.

Figure 9 describes the comparison of control performance between the control based on MTTE and MFC, as well as the non-control case.

Because the vehicle mass varies significantly in a real driving environment, In order to evaluate the robustness with variation in vehicle mass, some comparative experiments were performed with different nominal mass in the proposed controller while keeping the real vehicle mass fixed as 360 kg. Figure 10 provides these comparative results.

Figure 11 describes the results of the experiment with driving resistance. In these experiments, the driving resistance was simulated as 230 N, corresponding to the air resistance of a BMW 8-series running at a speed of 86 km/h, which is large enough for this experimental EV to evaluate the robustness on driving resistance.

Numerical simulation systems were done to provide more detailed comparisons and analysis, in which parameters could be set more precisely, providing finer insight into the controller behavior than is possible through experiments alone.

Figure 12 shows the simulation results in different slippery road conditions. In these simulations, the maximum friction coefficient of wet road was set to 0.6, and for icy road the coefficient was 0.3. The no-control case was assumed on the icy road.

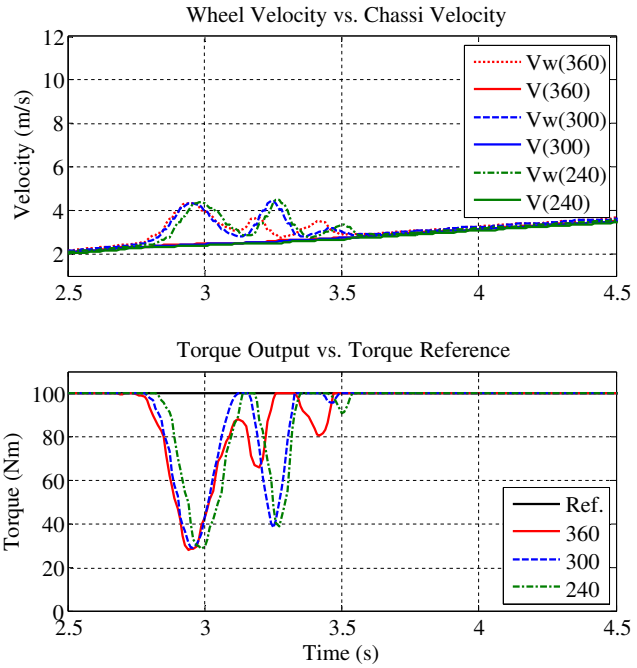

Fig. 10 Comparison of experimental results with variation in vehicle mass

Figure 13 shows the effect of the variation in the time constant in all LPFs, which share the same parameter. In these simulations, the time constants were varied from 20 ms to 80 ms, and the maximum friction coefficient was fixed at 0.3.

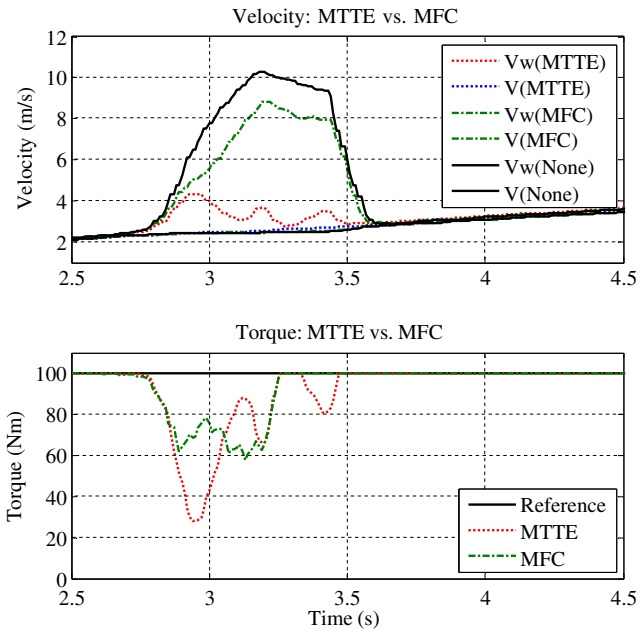

Fig. 9 Comparison of experimental results of two control design

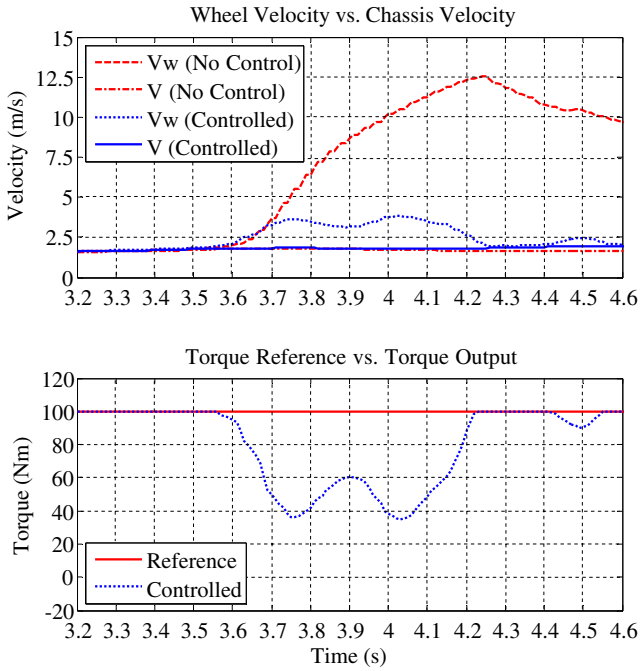

Fig. 11 Comparison of experimental results with driving resistance

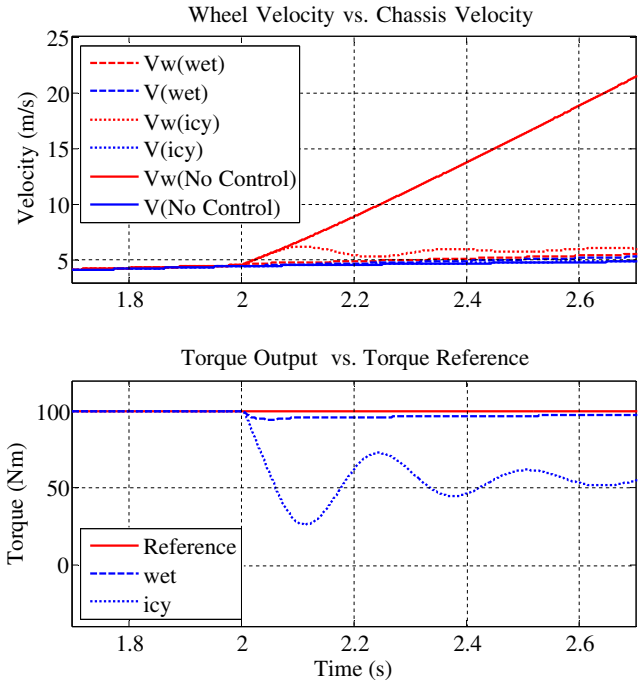

Fig. 12 Comparison of simulation results in different roads

In Fig. 14, small time constants in LPFs and small delay in electromechanical system were adopted to examine the relation between the friction force and the velocity difference, and α was set to 0.5. Here, the velocity difference, representing the extent of the slip, is equal to the difference between the wheel velocity and chassis velocity.

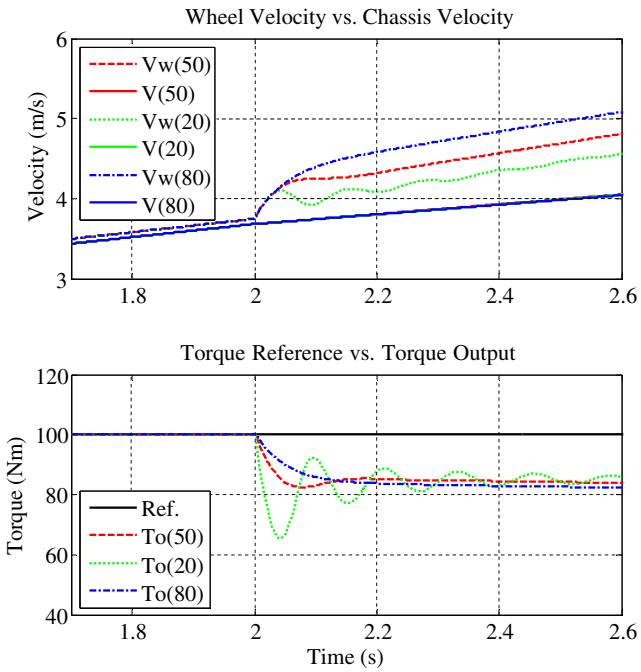

Fig. 13 Comparison of simulation results with variation in time constant

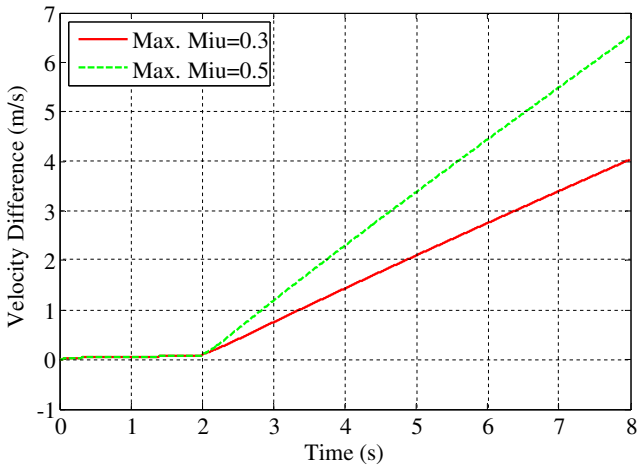

Fig. 14 Comparison of simulation results in different roads with small time constant

5 Discussion

Figures 9 and 12 show that, compared to the no-control case, the difference between the wheel velocity and the chassis velocity does not increase. The estimated maximum transmissible torque is close to the input reference torque for the normal road, and corresponds to the maximum friction force allowed by the slippery tire-road surface.

Figure 9 also shows that, compared with the control based on MFC, MTTE can provide better antislip control performance due to its use of a different control philosophy [21].

Figures 10 and 8 show that the proposed control system has high robustness to perturbations in vehicle mass and disturbances in driving resistance.

Figure 13 shows that the velocity difference between the wheel and the chassis is caused mainly by the delay in the control system. A shaft encoder with higher precision will decrease the system delay and provide higher antislip control performance. For the purpose of acquiring higher control performance, it is worthwhile to make every endeavor to decrease the system delay, for example, equipping more precise shaft encoders, adopting shorter sampling time, etc. However, LPF time constants which are too small will result in severe torque oscillation.

Moreover, the other experiments indicated that the larger the α, the better the antislip performance. However, an excessively large setting will raise possibility that the limiter does not work as expected [22].

Detailed analysis of control characteristics can be performed with a partially linearized vehicle model. When the control system operates in the closed-loop control state, if only the basic fact that the friction coefficient decreases with the velocity difference between the wheel and chassis is

considered, the whole controlled system can be simplified as in Fig. 15.

In Fig. 15, F_{do} is the friction force between the tire and road surface when antislip control starts. M_{n} denotes the nominal vehicle mass and generally it is equal to the mass of the vehicle and the driver. Here, it must be pointed out that in order to simplify the analysis, the delay in the vehicle system is ignored and the τ_2 is assumed equal to τ_1.

The transfer functions from F_{do} to A_{D} and from F_{dr} to A_{D} can be defined as T_{Ad} and T_{Ar} respectively, in which J is the equivalent system inertia.

$$J = J_w + Mr^2 \tag{10}$$

$$T_{Ad} = \frac{-J\tau_1 s^2 + \left(\frac{M}{\alpha M_n} - 1\right)J_w s}{MJ_w\tau_1 s^2 + (MJ_w - JK_u\tau_1)s + \left(\frac{M}{\alpha M_n} - 1\right)J_w K_u} \tag{11}$$

$$T_{Ad} = \frac{J_w\tau_1 s^2 + J_w s}{MJ_w\tau_1 s^2 + (MJ_w - JK_u\tau_1)s + \left(\frac{M}{\alpha M_n} - 1\right)J_w K_u} \tag{12}$$

Therefore, the steady state response of the system to inputs can be described as follows.

$$\lim_{t\to\infty} A_D(t) = \lim_{s\to 0} sT_{Ad}(s)F_{do}(s) + \lim_{s\to 0} sT_{Ar}(s)F_{dr}(s) \tag{13}$$

Here, the first item of Eq. (13) is used as an example to examine the relation between the friction force and the differential of the velocity difference as follows. F_{do} is assumed to be a step reference.

$$\lim_{s\to 0} T_{Ad}(s) < \lim_{s\to 0} \frac{-J\tau_1 s^2 + \left(\frac{M}{\alpha M_n} - 1\right)J_w s}{MJ_w\tau_1 s^2 + (MJ_w - JK_u\tau_1)s} = \frac{\frac{M}{\alpha M_n} - 1}{MJ_w - JK_u\tau_1}J_w \tag{14}$$

Equation (14) shows that the differential of the slip is proportional to the friction force, which agrees with the simulation results shown in Fig. 14. Moreover, when τ_1 and K_{u} are considerably larger, that is, the system delay cause the controller to be unable to follow the quickly varying friction force with the slip, the slip will become larger. This equation also indicates that the larger α, the better antislip performance.

Furthermore, if the vehicle mass can be known, then the estimated value of the friction force meaningfully reflects the tire-road conditions. This information can be sent to an ITS management center to construct a road information system, where vehicles in ITS, working as individual nodes, not only acquire transportation information from the system, but also share information with other vehicles.

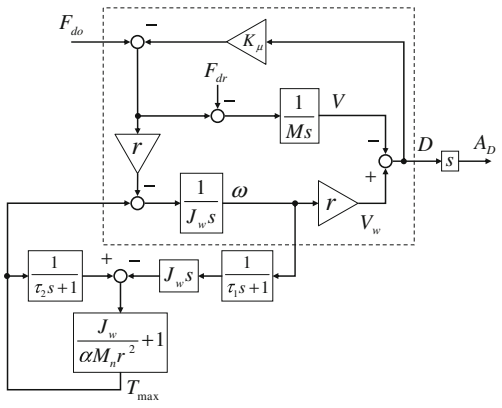

Fig. 15 Partially linearized control system

6 Conclusion

This paper proposed an estimator of the maximum transmissible torque and applied it to control the driving motors in EVs. The usefulness of the estimator indicated that the motor can act not only as a general actuator, but also as a measurement device because of its inherent features, which provides a good basis for antislip control as well as other more advanced motion control systems in vehicles.

The controller designed to co-operate with the estimator can provide higher antislip performance in a variety of tire-road conditions while maintaining stability. The comparative experiments and simulations with the variation of control variables proved the effectiveness and robustness of the proposed control design.

Additionally, it is possible for the controlled vehicle to share the road conditions obtained from the estimator with other vehicles in ITS.

Acknowledgments The authors wish to thank the engineers at AISIN AW CO., LTD. for their cooperation on the inverter modification; Eric Wu of Keio University and Jia-Sheng Hu of National Cheng Kung University for their advice on this manuscript. This research was supported by the Global COE in Secure-Life Electronics, the University of Tokyo.

References

1. Maier, M.W.: On architecting and intelligent transport systems. IEEE Trans. Aerosp. Electron. Syst. **33**(2), 510–625 (1997)
2. Takahashi, N., Tokunaga, R., Funahashi, M.: Development of road grip monitoring system. Proceeding of Symposium on ITS 2008, 103–108 (2008)
3. Liu, K., Yamamoto, T., Morikawa, T.: Study on the cost-effectiveness of a probe vehicle system at lower polling frequencies. International Journal of ITS Research **6**(1), 29–36 (2008)
4. Kodama, N., Hada, Y.: Road information gathering and sharing during disasters using probe vehicles. International Journal of ITS Research **6**(2), 97–104 (2008)
5. Bachmann, T., Naab, K., Reichart, G., Schraut, M.: Enhancing traffic safety with BMW's driver assistance approach connected drive. Proc. of Intelligent Transportation Systems Conference (2000)
6. Hoch, S., Schweigert, M.: The BMW SURF project: A contribution to the research on cognitive vehicles. Proceedings of the 2007 IEEE Intelligent Vehicles Symposium Istanbul (2007)
7. Pacejka, H.B., Bakker, E.: The magic formula tyre model. Veh. Syst. Dyn. **21**(1), 1–18 (1992)
8. Lee, H., Tomizuka, M.: Adaptive vehicle traction force control for intelligent vehicle highway systems (IVHSs). IEEE Transaction on Industrial Electronics **50**(1), 37–47 (2003)
9. Fujii, K., Fujimoto, H.: Traction control based on slip ratio estimation without detecting vehicle speed for EV. Fourth Power Conversion Conference-NAGOYA, pp. 688–693 (2007)
10. Chau, K.T., Chan, C.C., Liu, C.: Overview of permanent-magnet brushless drives for electric and hybrid EVs. IEEE Transaction on Industrial Electronics **55**(6), 2246–2257 (2008)
11. Affanni, A., Bellini, A., Franceschini, G., Guglielmi, P., Tassoni, C.: Battery choice and management for new-generation EVs. IEEE Transaction on Industrial Electronics **52**(5), 1343–1349 (2005)
12. Nagai, M.: The perspectives of research for enhancing active safety based on advanced control technology. Veh. Syst. Dyn. **45** (5), 413–431 (2007)
13. Hashimoto, N., Omae, M., Shimizu, H.: A study on reliable intelligent vehicle driving system by using features of EVs—lane keeping by traction-force-distribution control -. International Journal of ITS Research **1**(1), 25–31 (2003)
14. Hori, Y.: Future vehicle driven by electricity and control -research on four-wheel-motored "UOT Electric March II". IEEE Transaction on Industrial Electronics **5**, 954–962 (2004)
15. He, P., Hori, Y.: Optimum traction force distribution for stability improvement of 4WD EV in critical driving condition. Proc. of IEEE International Workshop on Advanced Motion Control, pp. 596–601 (2006)
16. Mutoh, N., Takahashi, Y., Tomita, Y.: Failsafe drive performance of FRID EVs with the structure driven by the front and rear wheels independently. IEEE Transaction on Industrial Electronics **55**(6), 2306–2315 (2008)
17. Sakai, S.-I., Hori, Y.: Advantage of electric motor for anti skid control of EV. European Power Electronics Journal **11**(4), 26–32 (2001)
18. Saito, T., Fujimoto, H., Noguchi, T.: Yaw-moment stabilization control of small EV. Proc. of Industrial Instrumentation and Control, IEE Japan, pp. 83–88 (2002)
19. Fujimoto H., Saito, T., Noguchi, T.: Motion stabilization control of EV under snowy conditions based on yaw-moment observer. Proc. of IEEE International Workshop on Advanced Motion Control, pp. 35–40 (2004)
20. Akiba, T., Shirato, R., Fujita, T., Tamura, J.: A study of novel traction control model for electric motor driven vehicle. Proc. of 4th Power Conversion Conference-NAGOYA, Conference Proceedings, pp. 699–704 (2007)
21. Yin, D., Oh, S., Hori, Y.: A novel traction control for EV based on maximum transmissible torque estimation. IEEE Transaction on Industrial Electronics **56**(6), 2086–2094 (2009)
22. Yin, D., Hori, Y.: A new approach to traction control of EV based on maximum effective torque estimation. Proceedings of The 34th Annual Conference of the IEEE Industrial Electronics Society, pp. 2764–2769, November 2008

Dejun Yin received the B.S. and M.S. degrees in electrical engineering from Harbin Institute of Technology, Harbin, China in 1999 and 2001 respectively. He received another M.S. degree in electronics engineering from Chiba Institute of Technology, Japan, in 2002, where he worked on embedded control system design in mechatronic engineering for nearly 5 years. In 2009, he received the Ph.D. degree from the Department of Electrical Engineering, the University of Tokyo, Japan.

He is currently a control specialist at Keio University, Japan, working on the development of vehicle control and motor design for EVs. He is a member of the Institute of Electrical Engineers of Japan, the Society of Automotive Engineers of Japan, and the IEEE Industrial Electronics Society.

Yoichi Hori received the B.S., M. S., and Ph.D. degrees in electrical engineering from The University of Tokyo, Tokyo, Japan, in 1978, 1980, and 1983, respectively. In 1983, he joined the Department of Electrical Engineering, The University of Tokyo, as a Research Associate. He later became an Assistant Professor, an Associate Professor, and, in 2000, a Professor. During 1991–1992, he was a Visiting Researcher at the University of California, Berkeley.